December 23, 2003

On the Self-Similarity of Unstable Magnetic Discontinuities in Solar Active Regions

Loukas Vlahos

Department of Physics,
University of Thessaloniki, 54 124 Thessaloniki, Greece

and

Manolis K. Georgoulis

The Johns Hopkins University Applied Physics Laboratory,
11100 Johns Hopkins Rd. Laurel, MD 20723-6099, USA

ABSTRACT

We investigate the statistical properties of possible magnetic discontinuities in two solar active regions over the course of several hr. We use linear force-free extrapolations to calculate the three-dimensional magnetic structure in the active regions. Magnetic discontinuities are identified using various selection criteria. Independently of the selection criterion, we identify large numbers of magnetic discontinuities whose free magnetic energies and volumes obey well-formed power-law distribution functions. The power-law indices for the free energies are in the range $[-1.6, -1.35]$, in remarkable agreement with the power-law indices found in the occurrence frequency distributions of solar flares. Our results show a strong self-similarity of the volumes that are likely to host flares and sub-flares, so the observed statistics of flares may only be the natural outcome of a previous spatial self-organization accompanying the energy fragmentation in solar active regions. We propose a dynamical picture of flare triggering consistent with recent observations by reconciling our results with the concepts of percolation theory and self-organized criticality. These concepts rely on self-organization, which is expected from the fully turbulent evolution of the magnetic fields in the solar atmosphere.

Subject headings: Sun:activity–Sun:magnetic fields–Sun:flares–Sun:active regions

1. Introduction

It is widely believed that magnetic fields and the dissipation of magnetic energy are responsible for the observed solar activity. Small-scale energy release, such as the "confined" flare (Moore et al. 1980) may be caused by the spontaneous formation of unstable magnetic discontinuities in solar active regions (ARs; Parker 1983, 1988). Magnetic discontinuities are formed and evolve either when the footpoints of the thin magnetic flux fibrils are moved and mixed by the continuous velocity field on the photosphere or when new magnetic flux emerges from the convection zone. The free (available for release) magnetic energy of these discontinuities is distributed through their volumes, which represent only a fraction of the total active-region volume. Magnetic energy dissipation is probably linked to a loss of equilibrium with respect to a *critical threshold*. This threshold might refer to, e.g., a critical current density j_c which, if locally exceeded, leads to current instabilities and heating due to the onset of anomalous resistivity (Papadopoulos 1977). The details of the above physical process are still unknown. Parker(1993) discussed the evolution and local reconstruction of the magnetic topology due to the anomalous resistivity. The formation of magnetic discontinuities and current sheets is a continuous process in ARs, independently of their productivity in flares and sub-flares. While most of these discontinuities remain relatively stable (sub-critical), a fraction of them may become unstable (critical), thus causing rapid magnetic reconnection, releasing their free magnetic energy and providing the energy content for a flaring or a sub-flaring event.

The concept of Self-Organized Criticality (SOC; see Bak 1996) refined the above picture significantly (Lu & Hamilton 1991; Vlahos et al. 1995): An internal self-organization in solar ARs leads to the formation of a network of minimally stable magnetic structures. If one of these structures becomes unstable, it triggers a cluster of instabilities causing an avalanche-type energy release event. In the course of an avalanche, previously sub-critical configurations may become critical, thus increasing exponentially the flaring volume. The crucial elements in constructing a dynamical picture of flare triggering were already in place before the introduction of SOC (i.e., critical thresholds, magnetic reconnection and field restructuring, anomalous resistivity and heating), but the missing link was the non-linear formation of an avalanche. The outcome of SOC is scale-invariance and extended power laws in the predicted frequency distributions of flare sizes, in concert with the observations of Crosby, Aschwanden, & Dennis (1993) and numerous authors thereafter.

Occasionally, an avalanche may cause a global destabilization of the active-region magnetic field structure, thus leading to an *ejective* flare (Svestka 1986) which might eventually drive a coronal mass ejection via, e.g., the *breakout model* (Antiochos, DeVore, & Klimchuk 1999). The morphological diversity of the energy release process cannot be summarized to

just a few flare categories. Nevertheless, a number of characteristic magnetic topologies have been traditionally viewed as sources of very large flares, such as the extended sheared arcades that provide a *two-ribbon* flare or filament eruptions (see Priest & Forbes (2002) and references there in). These rare flares are not the subject of the present study, which focuses on the confined, small-scale events.

A possible self-organization of the magnetic structures on the photosphere has been revealed in numerous statistical studies (see Howard (1996) and references therein) and is reflected by their fractal character (Meunier 1999). Percolation theory, known to reasonably reproduce the formation of solar ARs (Seiden & Wentzel 1996; Vlahos et al. 2002; Fragos, Rantsiou, & Vlahos 2004), might account for these observations. Percolation is another self-organized (although non-critical) process and implies that the footpoint motion on the photosphere is probably not a random walk, as assumed repeatedly in the literature, but a more complex process dictated by the fractality of the magnetic energy fragmentation.

In this study we investigate the possible self-organization of the magnetic field discontinuities in active-region atmospheres focusing on the three-dimensional *non-flaring* magnetic structure of solar ARs. We use several different selection criteria to identify potentially unstable locations and we apply standard linear force-free extrapolations to calculate the magnetic field configurations in solar ARs. We perform the analysis in two ARs observed by the Mees Solar Observatory's Imaging Vector Magnetograph (IVM; Mickey et al. 1996). The description of the method is provided in §2. In §3 we apply the method to the IVM data and we describe the results. In §4 we discuss the implications of our findings.

2. Analysis method

Calculation of the coronal magnetic field: Starting from an observed active-region vector magnetogram, *(i)* we resolve the intrinsic azimuthal ambiguity of 180^o, and *(ii)* we find the best-fit value α_{AR} of the force-free parameter for the entire AR. The 180^o-ambiguity is resolved by means of the "structure minimization" method of Georgoulis, LaBonte, & Metcalf (2004). The best-fit α_{AR} is calculated using the "minimum residual" method of Leka & Skumanich (1999), i.e. by minimizing the difference between the extrapolated and the ambiguity-resolved observed horizontal magnetic fields. We then perform a linear force-free extrapolation (Alissandrakis 1981) to determine the three-dimensional magnetic field in the AR. Although it is known that the magnetic fields on the photosphere are not force-free (Georgoulis & LaBonte 2004), we feel that a linear force-free approximation is suitable for our statistical purposes.

Selection criteria: We apply two different selection criteria in order to identify potentially unstable locations. These criteria refer to *(i)* Parker's angle, and *(ii)* the total magnetic field gradient. The angular difference $\Delta\psi$ between two adjacent magnetic field vectors, $\mathbf{B_1}$ and $\mathbf{B_2}$, is given by

$$\Delta\psi = cos^{-1}(\frac{\mathbf{B_1}\cdot\mathbf{B_2}}{B_1 B_2}) \ . \tag{1}$$

Assuming a cubic grid, we calculate six different angles at any given location, for each of this location's closest neighbors. The location is considered potentially unstable if at least one angle $\Delta\psi_i$; $i \equiv \{1,6\}$ is larger than $\Delta\psi_c = 14^o$. The "critical" value $\Delta\psi_c$ refers to the Parker's angle which, if exceeded, favors tangential discontinuities and the triggering of fast reconnection (Parker 1983, 1988).

The total magnetic field gradient between two adjacent locations with magnetic field strengths B_1 and B_2 is given by $\frac{|B_1-B_2|}{B_1}$. We calculate six different gradients at any given location. If at least one gradient is larger than a preset value of $G_c = 0.2$, then the location is considered potentially unstable. A steep gradient of the magnetic field strength is thought to favor magnetic reconnection in three dimensions, in the absence of null points (Priest, Hornig, & Pontin 2003). **Estimation of the free magnetic energy**: Potentially unstable volumes are formed by adjacent selected locations. These volumes are given by $V = N\lambda^2 h$, where N is the number of adjacent locations, λ is the pixel size of the observed magnetogram and h is the height step of the force-free extrapolation. The *free* magnetic energy E in any volume V is given by

$$E = \frac{\lambda^2 h}{8\pi}\sum_{l=1}^{N}(\mathbf{B_{ff}}_l - \mathbf{B_p}_l)^2 \tag{2}$$

where $\mathbf{B_{ff}}_l$ and $\mathbf{B_p}_l$ are the best force-free field and the potential field at location l, respectively. The assumption used is that any deviation from a potential configuration implies a non-zero free magnetic energy which is likely to be released if certain conditions are met.

3. Results

The above method is applied to two timeseries of active-region vector magnetograms, namely for NOAA ARs 9114 and 9165, observed by IVM on 8 August 2000 and 15 September 2000, respectively. The timeseries span over several hr, corresponding to the IVM daily observing interval (from ∼17:30 UT to ∼22:30 UT). No significant flaring activity was recorded in NOAA AR 9114 during the observations. NOAA AR 9165 was more dynamic, showing a number of sub-flares but no major flares. By choosing the above ARs we illustrate that the statistical behavior of the magnetic discontinuities is common and independent of the

flare productivity in the AR. Extrapolations proceed up to a height of 100 Mm, with a step height $h = 0.1\ Mm$. The IVM pixel size is $\lambda = 0.55\ arcsec \simeq 0.396\ Mm$ and hence a volume element in our calculation is $\sim 0.016\ Mm^3$.

Figures 1a and 1c show snapshots of the three-dimensional magnetic topology in NOAA ARs 9114 and 9165, respectively. In Figure 1b we show a small portion of the atmosphere of Figure 1a, up to a height of 7 Mm. We identify 2394 potentially unstable volumes shown for a Parker angle $\Delta\psi_c = 10^o$ (green) and $\Delta\psi_c = 8^o$ (blue). For altitudes larger than 7 Mm the smooth products of the extrapolation preclude the fulfillment of any of the selection criteria discussed in §2.2. A similar situation exists at any given time for both ARs. In Figure 1d we show the photospheric projection of 1387 potentially unstable volumes identified in NOAA AR 9165 with a Parker angle $\Delta\psi_c = 14^o$ (red) and 2834 volumes identified with a total field gradient $G_c = 0.2$ (green). The blue areas indicate locations where both criteria are satisfied.

A typical distribution function of the total free energy in the selected volumes is given in Figure 2a. We obtain a well-defined power law extending over two orders of magnitude in the range $[10^{24}\ ,\ 10^{26}]\ erg$, with power-law index $\alpha_E = -1.37 \pm 0.12$. Notice the close proximity of the power-law index with that of the total energy distribution of flares, known to vary between -1.4 and -1.6. If avalanches involve a random sample of these volumes, the total-energy frequency distribution of the resulting flares should not be very different from the distribution of Figure 2a. The selected volumes also obey a power-law frequency distribution such as the one shown in Figure 2b. The power-law index is $\alpha_V = -1.45 \pm 0.19$. The non-integer value of the index α_V illustrates the spatial fractality of the energy fragmentation process (McIntosh & Charbonneau 2001).

Figure 3a shows the variability of the power-law indices α_E over the entire observing interval when a Parker's angle $\Delta\psi_c = 14^o$ is used as the selection criterion. The points and error bars correspond to NOAA AR 9114, while the mean index values $< \alpha_E >$ are shown with straight lines for both ARs. Although the error bars are not negligible, no systematic tendency with time is obvious in the values of α_E. The mean values $< \alpha_E >$ for NOAA ARs 9114 and 9165 are -1.35 ± 0.16 and -1.50 ± 0.18, respectively. Using a total field gradient $G_c = 0.2$ as the selection criterion, we obtain $< \alpha_E >= -1.50 \pm 0.23$ and $< \alpha_E >= -1.61 \pm 0.1$ for NOAA ARs 9114 and 9165, respectively. All indices are in excellent agreement with numerous flare observations. Of particular interest is whether power-law indices change when the critical thresholds used in the selection criteria of §2.2 change. In Figure 3b we have performed this test for both ARs for different definitions of the Parker's angle $\Delta\psi_c$. Very similar results are obtained when the threshold G_c of the total field gradient changes. Although within error bars, we find a weak dependence between $< \alpha_E >$ and $\Delta\psi_c$. For lower $\Delta\psi_c$, when the number of selected volumes increases and the

total free energy distribution extends mostly toward lower energies, the power-law indices become steeper. This might favor a nanoflaring scenario with a background of numerous small events obeying steeper power laws, but clearly more investigation is required on this point. For moderate changes of $\Delta\psi_c$ centered around the value of 14^o, $< \alpha_E >$ is very consistent with flare observations.

4. Discussion and Summary

We present evidence of strong self-similarity of the possible magnetic discontinuities in solar ARs. These potentially unstable volumes may well be self-organized, as suggested by percolation and SOC concepts used to describe the formation and evolution of ARs. This study suggests that the intrinsic self-similarity found in the distribution functions of flare parameters is a direct outcome of the self-similarity of the volumes hosting the flares. Using standard linear force-free extrapolations we find that *(i)* a complex network of potentially unstable volumes are present in both studied ARs at any given time, independently of their activity and for the entire observing interval of several hr, *(ii)* these volumes are preferentially located close to the photosphere which suggests that energy release might be enhanced at low latitudes (Aschwanden, Schrijver, & Alexander 2001), *(iii)* the distribution functions of these volumes as well as of their total free energies are well-formed power laws with indices $\alpha_V \simeq -1.5$ and $\alpha_E \in [-1.6, -1.35]$, respectively, *(iv)* the above power-law indices depend weakly on the selection criterion and the critical threshold, with a tendency to become flatter as the selection criterion becomes more stringent, and *(v)* the maximum free energies of the selected volumes are of the order $\sim 10^{27}\ erg$. This implies a non-linear interaction of a large number of volumes to provide a large flare with energy, say $\sim 10^{30} erg$, suggestive of a SOC-type avalanche analogue or of a "tectonic" behavior in *magnetic separatrices* (Démoulin & Priest 1997), as discussed by Schrijver & Title (2002).

Critical and non-critical self-organization may be essential for the formation and evolution of solar ARs. While non-critical self-organization (e.g. percolation) may regulate the emergence and evolution of magnetic fields in the solar atmosphere, critical self organization (e.g. SOC) may determine the energy release process. The nature of the critical threshold(s) (electric current density, angular difference, field strength gradient) remains elusive. Energy release in the form of flares cannot be accomplished unless non-linear interaction or intercommunication between individual energy release sites is at work. In essence, solar ARs are an externally driven, self-organized non-linear dynamical system, subject to a self-similar external driver such as the one modeled by Georgoulis & Vlahos (1996, 1998). Energy release can occur anywhere in the atmosphere, from the photosphere to the corona, and it might

be enhanced at low altitudes according to the situation (see e.g., the discussion of Priest, Heyvaerts, & Title 2002). Self-organization and the cascading nature of solar flares are the natural outcome of the fully-developed turbulence acting in the solar atmosphere (Biskamp 1993; Einaudi et al. 1996).

As a simple paradigm, the free magnetic energy in an AR may be viewed as a warehouse storing explosives. The spatial distribution of the explosives inside the warehouse is crucial when a fire breaks out at one particular spot. If this spot is isolated, the explosion will be small-scale and the damage will be insignificant. If stacks of explosives exist near the spot of the initial explosion, then a chain reaction will occur and the entire stock will be destroyed almost instantly. This scenario was proposed for the interpretation of solar flares twenty years ago (Vlahos et al. 1984) and it might still serve as a valid working hypothesis.

We are grateful to B. J. LaBonte, for kindly providing us with the IVM magnetograms. Data used here from Mees Solar Observatory, University of Hawaii, are produced with the support of NASA and AFRL grants. This work has received partial support by NSF grant ATM-0208104 and by the Research Training Network (RTN) "Theory, Observation and Simulation of Turbulence in Space Plasmas", funded by the European Commission (contract No. HPRN-eT-2001-00310).

REFERENCES

Alissandrakis, C. E., 1981, A&A, 100, 197

Antiochos, S. K., DeVore, C. R. & Klimchuk, J. A., 1999, ApJ, 510, 485

Aschwanden, M. J., Schrijver, C. J., & Alexander, D., 2001, ApJ, 550, 1036

Bak, P., 1996, How Nature Works, Springer Verlag: New York

Biskamp, D., 1993, Nonlinear Magnetohydrodynamics, Cambridge University Press: Cambridge

Crosby, N. B., Aschwanden, M. J., & Dennis, B. R., 1993, SoPh, 143, 275

Démoulin, P., & Priest, E. R., 1997, SoPh, 175, 123

Fragos, T., Rantsiou, M., & Vlahos, L., 2004, A&A, in press

Georgoulis, M. K., & LaBonte, B. J., 2004, ApJ, submitted

Georgoulis, M. K., LaBonte, B. J., & Metcalf, Th. R., 2004, ApJ, in press

Georgoulis, M. K., & Vlahos, L., 1996, ApJ, 469, L135

Georgoulis, M. K., & Vlahos, L., 1998, A&A, 336, 721

Einaudi, G., Velli, M., Politano, H., & Pouquet, A., 1996, ApJ, 457, L113

Howard, R.F., 1996, ARA&A, 34,75

Leka, K. D., & Skumanich, A., 1999, SoPh, 188, 3

Lu, E. T., & Hamilton, R. J., 1991, ApJ, 380, L89

McIntosh, S. W., & Charbonneau, P., 2001, ApJ, 563, L135

Meunier, N., 1999, ApJ, 515, 801.

Mickey, D. L., Canfield, R. C., LaBonte, B. J., Leka, K. D., Waterson, M. F., & Weber, H. M., 1996, SoPh, 168, 229

Moore, R., et al., 1980, In Solar Flares: A Monograph from Skylab Solar Workshop II (ed.: Sturrock, P.), Colorado Associated University Press:Boulder, p. 341

Papadopoulos, K., 1977, Rev. Geoph. Spac. Phys., 15, 113

Parker, E. N., 1983, ApJ, 264, 642

Parker, E. N., 1988, ApJ, 330, 474

Parker, E.N., 1993, ApJ, 414, 389

Priest E. R., & Forbes, T. G., 2002, A&A Rev., 10, 313

Priest, E. R., Heyvaerts, J. F. & Title, A. M., 2002, ApJ, 576,533

Priest, E. R., Hornig, G., & Pontin, D. I., 2003, J. Geoph. Res. Space Phys., 108, A7, 1285

Schrijver, C. J., & Title, A. M., 2002, SoPh, 207, 223

Seiden, P. E., & Wentzel, D.G., 1996, ApJ, 460, 522

Svestka, Z., 1986, In The Lower Atmosphere of Solar Flares (ed.: Neidig, D. F.), Tuscon, Arizona, p. 332

Vlahos, L., et al., In Energetic phenomena on the Sun (eds.: Kundu, M. & Woodgate, B.), NASA Conference Publication 2439

Vlahos, L., Georgoulis, M., Kluiving, R., & Paschos, P., 1995, A&A, 299, 897

Vlahos, L., Fragos, T., Isliker, H., & Georgoulis, M., 2002, ApJ, 575, L87

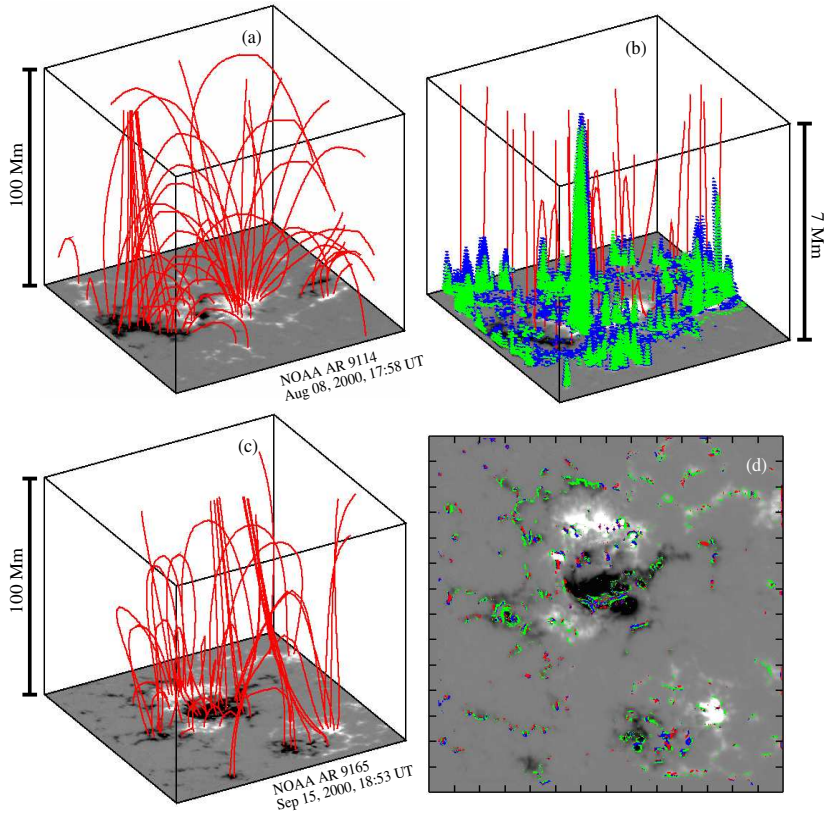

Fig. 1.— (a) Snapshot magnetic field configuration in NOAA AR 9114. Linear force-free extrapolation proceeds up to a height of 100 Mm with a force-free parameter $\alpha_{AR} = -1.39 \times 10^{-2}\ Mm^{-1}$. (b) A part of the atmosphere for NOAA AR 9114, up to a height of 7 Mm. Shown are the magnetic field lines (red), with the identified magnetic discontinuities for a Parker angle $\Delta\psi_c = 10^o$ (green) and $\Delta\psi_c = 8^o$ (blue). (c) Snapshot magnetic field configuration in NOAA AR 9165. Linear force-free extrapolation proceeds up to a height of 100 Mm with a force-free parameter $\alpha_{AR} = -1.89 \times 10^{-2}\ Mm^{-1}$. (d) Projection of the identified magnetic discontinuities on the photosphere for NOAA AR 9165. The selection criteria are a Parker angle $\Delta\psi_c = 14^o$ (red) and a total field gradient $G_c = 0.2$ (green). Some selected locations satisfy both criteria (blue). Tic mark separation is $20''$.

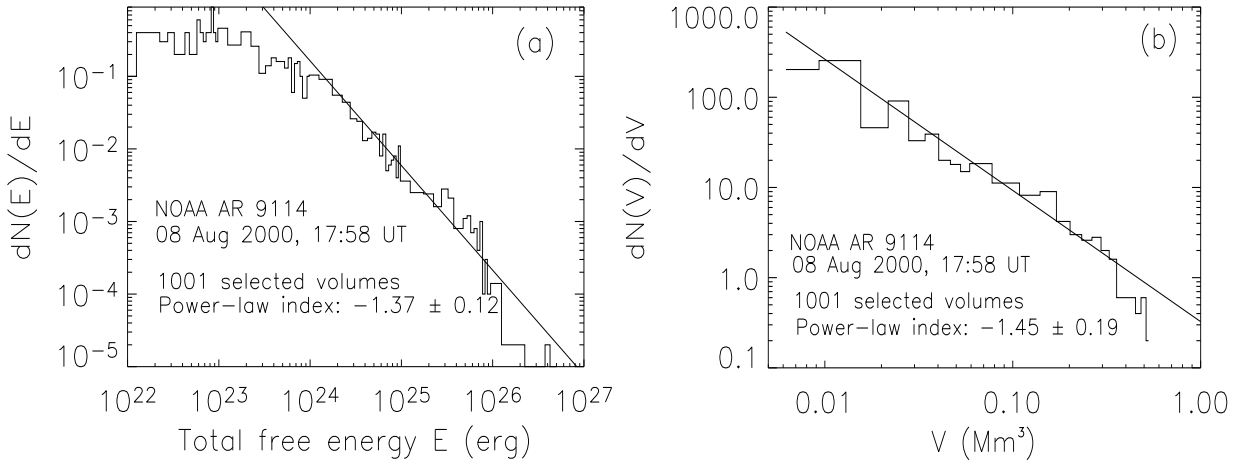

Fig. 2.— (a) Typical distribution function of the total free energy in volumes selected using a Parker angle $\Delta\psi_c = 14^o$. (b) The respective distribution function of the selected volumes.

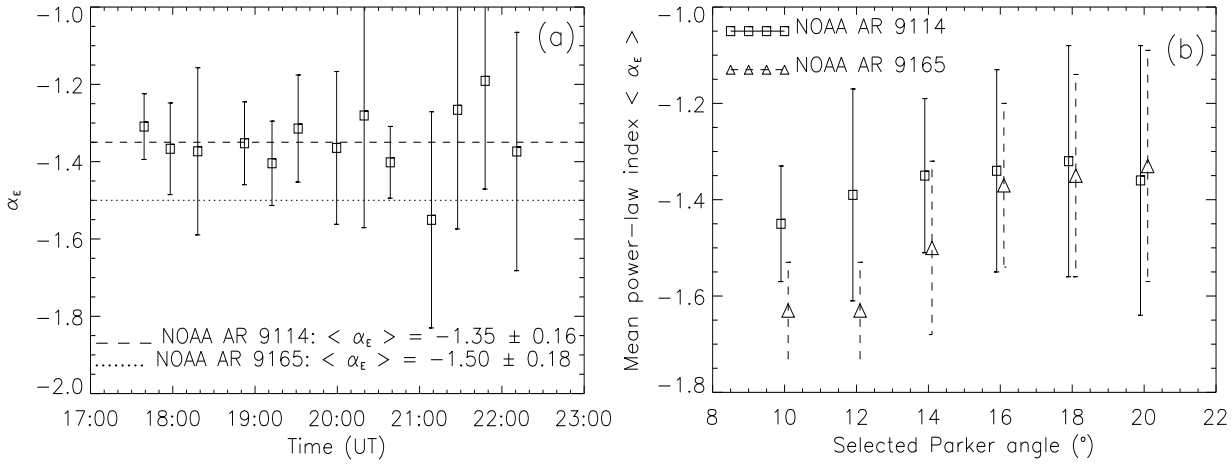

Fig. 3.— (a) Temporal variability of the power-law indices over the IVM observing interval. Statistics have been obtained using a Parker angle $\Delta\psi_c = 14^o$. The points and error bars correspond to NOAA AR 1914. The mean power-law indices $< \alpha_E >$ are indicated by a dashed line (NOAA AR 9114) and by a dotted line (NOAA AR 9165). (b) The mean power-law index $< \alpha_E >$ for different definitions of the Parker angle. Rectangles and solid error bars correspond to NOAA AR 9114. Triangles and dashed error bars correspond to NOAA AR 9165.